UAV Icing: Comparison of LEWICE and FENSAP-ICE for Anti-Icing Loads

Richard Hann [1]
Norwegian University of Science and Technology (NTNU), Trondheim, 7034, Norway

One of the main operational limits for UAV operations today is atmospheric icing. Icing degrades the aerodynamic performance by reducing lift, increasing drag and reducing stall margins. To extend the operational envelope to icing conditions, UAVs require the development of suitable icing protection systems. While such systems are standard in manned aviation, very few systems exist for UAVs. In this study, FENSAP-ICE and LEWICE, two numerical icing codes that have been developed for general aviation, will be compared in their capability to assist in the design process for a UAV anti-icing protection system. First, the required heat fluxes to keep the surface of a typical UAV airfoil clean of ice are simulated for several meteorological icing conditions. Two operational modes, running wet and fully evaporative, are evaluated in 2D. The results indicate moderate differences in convective and evaporative heat transfer. The comparison of the total heat requirements between the two modes reveals that both may be beneficial in certain conditions. For the simulation of running wet, FENSAP-ICE displays a sensitivity for laminar-turbulent transition which may play a much larger role for UAVs compared to general aviation applications. Second, simulations on a wing are performed in 3D with FENSAP-ICE and compared to equivalent 2D cross-sections in LEWICE. The simulations show a small influence of 3D flow and the wing-tip vortex on the required heat loads. Generally, LEWICE and FENSAP-ICE estimates show good consistency with only moderate deviations in some cases. The results of this study are not validated against experimental results and serve therefore only as a first assessment of UAV anti-icing loads.

I. Nomenclature

α	=	angle of attack
Λ	=	wing aspect ratio
b	=	wing span
c	=	chord
LWC	=	liquid water content
MVD	=	droplet median volume diameter
Re	=	Reynolds number
RH	=	relative humidity
q	=	heat flux
s	=	wrap distance
T	=	temperature
v	=	velocity

II. Introduction

Atmospheric icing imposes a significant limitation on the operational envelope of unmanned aerial vehicles (UAVs) (Siquig, 1990). While there is a good understanding of icing for general aviation (Bragg et al., 2005), few studies discuss icing on UAVs. The existing studies indicate that icing on a UAV degrades its aerodynamic performance by reducing lift, increasing drag and negatively affecting the stall behavior (Hann, 2018; Hann et al., 2017; Szilder and Yuan, 2017; Tran et al., 2004; Williams et al., 2017). All these factors constrain the flight envelope and significantly increase the risk of losing the aircraft. In order to mitigate the adverse effects of icing, icing protection

[1] PhD Candidate, Norwegian University of Science and Technology, Centre for Autonomous Marine Operations and Systems (NTNU-AMOS), O. S. Bragstads plass 2D, 7034 Trondheim, Norway. E-mail: richard.hann@ntnu.no

systems (IPS) are required. Whereas for commercial and military aviation a wide range of mature icing protection systems exists (Goraj, 2004), such solutions are very limited for UAVs.

This study focuses on fixed-wing UAVs with wing-spans of several meters. These UAVs are suited for many autonomous applications, for example for remote sensing, search and rescue, oil spill detection, ship-based iceberg tracking, etc. (Hann, 2017). Typical mission profiles require the capability to operate autonomously, beyond line of sight, for extended periods, in all weather conditions. Atmospheric in-cloud icing imposes a significant barrier to the ability of a UAV to execute the aforementioned tasks. Essentially, UAVs today are grounded during icing conditions or face a substantial risk of losing control and crashing. Therefore, developing a suitable IPS for UAVs is one of the key challenges for the successful use of autonomous fixed-wing UAVs in the future.

A multitude of IPS solutions exists for manned aviation (Goraj, 2004), but they are only partly transferable to UAVs. There are several key differences between manned and unmanned aircraft. UAVs are typically smaller in size. This implies that there are more strict weight and dimensional constraints to an IPS. Consequently, power is a limited resource on UAVs which means that an IPS needs to be particularly energy efficient. The only available energy form is usually electric. Icing detection on a UAV needs to be fully autonomous, without any visual information from a human pilot (Sørensen, 2016). The instrumentation for detection should be minimal and energy efficient. Last but not least, UAVs are less cost-intensive compared to manned aircraft, which means that smaller budgets are available for IPS development. On a side note, many of these characteristics can be found in cold climate wind energy (Battisti, 2015).

For the development of manned aircraft, much more resources in design, engineering, and testing are available than for UAVs. Normally, experiments in icing wind tunnels are performed as part of the IPS design and certification process (Federal Aviation Administration, 2002). Such experiments are very expensive and time-consuming. Therefore, they might not be affordable in the scope of a UAV development program. A cheaper method to design an IPS is by using numeric simulation tools. This paper aims to compare the suitability of two icing codes for the purpose of designing a UAV IPS. It is important to note that most numerical models have been developed for the high Reynolds numbers of general aviation ($Re > 2 \times 10^6$) whereas UAVs typically operate in a lower Reynolds regime ($Re < 2 \times 10^6$). This can have a significant impact on the ice accretion process (Szilder and McIlwain, 2011), but also on flow characteristics. In particular, laminar boundary layer effects are going to be more dominant at lower Reynolds numbers (Schlichting, 1968).

In the scope of this study, an electro-thermal anti-icing system is considered. This type of system provides heat to specially coated areas on the wing via electric currents. Electro-thermal systems are well-suited for UAVs, as they are light-weight and require only electrical power, which is often easily available – although limited in amount. Anti-icing systems continuously supply heat in order to avoid ice accretion on critical surfaces (Gent and Cansdale, 2000). Generally, there are two different operation modes of such an IPS. Systems are called *fully evaporative* if the provided heat is sufficient to evaporate the incoming liquid water within the impingement zone. The advantage of a fully evaporative system is that it has no risk for runback icing and the area to be protected is limited. On the draw-back, such systems require high heat fluxes and may result in exceedingly high surface temperatures. An anti-icing system is considered to be *running wet* when it is providing just enough heat to prevent super-cooled droplets from freezing on the surface. Running wet anti-icing systems typically require a larger area to be heated, but with lower heat fluxes and lower surface temperatures. The resulting water film from a running wet system may freeze downstream of the heated areas and form runback ice that can have severe effects on the aerodynamics (Bragg et al., 2005; Whalen, EA; Broeren, AP; Bragg, 2007). In contrast, de-icing systems allow for limited amounts of ice to build up which are removed periodically with short high-energy bursts. $\bar{x}$

III. Numerical Tools

Two numerical tools will be used to assess IPS loads. LEWICE (version 3.2.2) is a widely used first-generation icing tool based on a 2D panel-method (Wright, 2008). LEWICE has been developed by NASA and has been validated over a wide range of parameters with extensive experimental icing wind tunnel data (Wright and Rutkowski, 1999). LEWICE is formally only validated in a high Reynolds number regime ($Re > 2.3 \times 10^6$) (Wright, 2008), but it may still be practically used for lower Reynolds numbers (Hann, 2018). The 2D panel-method in LEWICE has very low computational requirements which allows LEWICE to obtain a large number of results in a short time. This feature is well suited to study a wide range of icing parameters to gain a better understanding of the dominating variables in a specific icing scenario. Such a characteristic is particularly relevant for designing an efficient IPS with regards to investigating different cases, configurations, heat requirements, etc. However, because a panel-method captures many of the physical processes by means of (theoretical or experimental) correlation, the simulation of anti-icing loads needs to be validated. In absence of relevant experimental data for UAVs, LEWICE will be compared to a higher order code.

ANSYS FENSAP-ICE (version 19.2) is a second-generation, state-of-the-art computational fluid dynamics (CFD) icing code, capable of 2D and 3D icing simulations for a large variety of applications (Habashi et al., 2004). The code consists of separate modules that aim to directly capture the main physical icing and heat transfer processes (Morency et al., 2001; Reid et al., 2011): the flow field is simulated with a Reynolds-Averaged Navier-Stokes (RANS) flow solver; droplet and ice crystal impingement are simulated using a Eulerian approach; ice growth is captured by solving the partial differential equations (PDEs) on the iced geometry.

All CFD flow calculations in FENSAP-ICE are performed by using a steady-state method with streamline upwind artificial viscosity. Turbulence is implemented with a Spalart-Allmaras (turbulent) or K-omega SST (intermittent transition) model. The discretization for CFD is executed as hybrid O-grids with a structured resolution of the boundary layer and an unstructured far field.

IV. Method

In this paper, two different approaches are pursued to compare the IPS capabilities of LEWICE and FENSAP-ICE on UAVs. First, the required heat fluxes for a running wet and fully evaporative anti-icing system are compared on a 2D airfoil for three different meteorological cases. Second, the anti-icing loads for a selected icing case are evaluated on a 3D wing. FENSAP-ICE fully simulates the wing whereas LEWICE evaluates four 2D cross-sections of the wing.

The HQ/DS-2.5/13 airfoil is chosen as a base 2D geometry. It has been developed for dynamic soaring of gliders at low Reynolds numbers ($Re < 1 \times 10^6$) (Quabeck, 2014). This makes the airfoil suitable for may UAV applications and has been considered for several airframe designs. For the 3D wing case, a simple wing using the HQ/DS-2.5/13 airfoil with a span of $b = 1.5\text{m}$, aspect ratio of $\Lambda = 4.7$ and a straight trailing edge is used, see Fig. 4.

The task of finding relevant meteorological design cases serves as an example of how LEWICE can be used to quickly investigate a larger number of cases. The entire CFR 14, Part 25, Appendix C icing envelope for continuous maximum icing conditions (Federal Aviation Administration, 2002) is used for a parameter study. The boundary (min/max) conditions are listed in Table 1. The running wet heat fluxes for 128 different cases were calculated with LEWICE in about 20 minutes on a standard office laptop, shown in Fig. 1. From this, three icing cases that seemed interesting with respects of required heat and impingement limits have been chosen to be investigated and are presented in Table 1. Case A represents the highest required anti-icing loads, Case B exhibits a large impingement zone and the most runback, and Case C is an example of icing during take-off or landing.

Table 1. Icing test cases.

Parameters	*min/max*	*Case A*	*Case B*	*Case C*
Velocity $\boldsymbol{v_{icing}}$	20 – 25 m/s	25 m/s	25 m/s	20 m/s
Angle of attack $\boldsymbol{\alpha_{icing}}$	0 – 4°	0°	0°	4°
Relative Humidity $\boldsymbol{RH}$	100 %	100 %		
Chord $\boldsymbol{c}$	0.40 m	0.40 m		
Droplet $\boldsymbol{MVD}$	15 – 40 µm	15 µm	40 µm	20 µm
Liquid water content $\boldsymbol{LWC}$	0.04 – 0.76 g/m³	0.20 g/m³	0.13 g/m³	0.43 g/m³
Temperature $\boldsymbol{T_{icing}}$	-2 – -30 °C	-30 °C	-4 °C	-10 °C

V. Results

The required heat fluxes on a running wet IPS for the HQ/DS-2.5/13 airfoil are shown in Fig. 2 for both numerical codes. The horizontal axis represents the dimensionless wrapping distance from the leading-edge, with negative values indicating the bottom-side of the airfoil. The vertical axis shows the required heat flux to maintain a surface temperature of 0°C and to prevent any ice formation. In order to show the influence of transition, FENSAP-ICE calculations are performed fully turbulent (*turb*) and using the k-omega SST intermittency transition model (*trans*).

Three distinct zones can be identified in each graph. First, the highest heat requirements occur close to the stagnation point at the leading-edge of the airfoil. In this area, the super-cooled cloud droplets collide with the airfoil and require high energy fluxes to prevent instantaneous freezing. The magnitude of this initial heat spike is mainly depending on the droplet and ambient temperature and is, therefore, highest for Case A ($T_{Droplet} = -30°\text{C}$) and lowest for Case B ($T_{Droplet} = -4°\text{C}$). Since flow velocities are low, the role of stagnation point heating is minor.

The second area is defined by heat transfer on a wetted surface. The incoming droplets form a water film on the surface that is transported downstream due to aerodynamic friction. In addition to the convective heat transfer, evaporation cooling needs to be compensated by the anti-icing system. The limits of this wet zone are defined by the

location where the liquid water film is completely removed. When the surface becomes dry, a sudden *decrease* of the required heat occurs (e.g. at $s/c = \pm 0.1$ in Fig. 2a, or at $s/c = -0.7$ in Fig. 2b for FENSAP-ICE turbulent). This represents the third zone, where the surface is dry, and the required heat flux is driven by compensating the convective

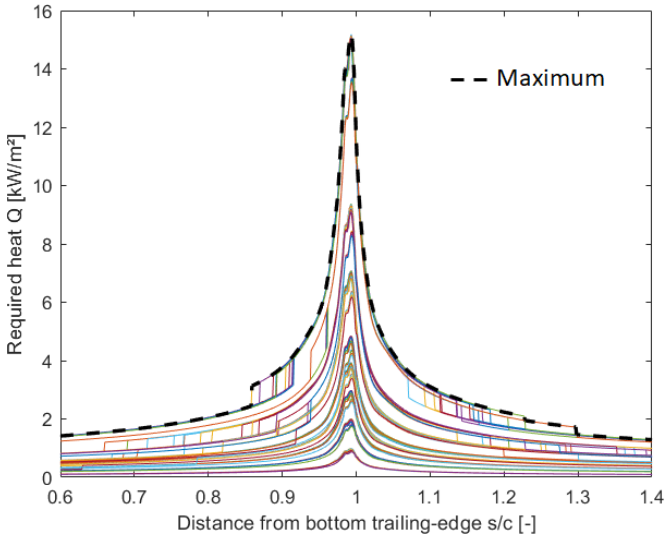

Fig. 1. Required anti-icing heat fluxes for running wet operation from LEWICE for 128 cases.

heat transfer. Technically this energy is not required for the anti-icing system (waste heat), but it serves as an indicator of the heat transfer model in LEWICE and FENSAP-ICE. A steep *increase* of the required heat flux in the dry or wet zone for the FENSAP-ICE transition results indicates the location of the laminar-turbulent transition point. A turbulent boundary layer increases convective heat transfer due to higher turbulence (Kays et al., 2005). An increase in heat flux cannot be detected for LEWICE, indicating that the code does not predict laminar-turbulent transition in any of the three cases.

The green curve in Fig. 2c serves as an example to describe the three thermodynamic regimes. At the leading-edge, the heat transfer is the highest due to incoming droplets. A thin water film will build on the upper side of the airfoil with laminar heat transfer. The laminar-turbulent transition is predicted at $s/c = 0.7$, which is consistent with XFOIL simulations (Drela, 1989). Downstream of this point, the flow becomes turbulent and increases heat transfer due to increased energy transport in the boundary layer. This accelerates evaporation rates and increases the required heat fluxes. Consequently, at $s/c = -0.85$, the water film disappears, and turbulent convective heat transfer becomes dominant on the dry surface. Without evaporation, the heat requirements are reduced.

For the running wet results, LEWICE predicts larger heat spikes in the impingement area whereas the location and extent are almost identical to FENSAP-ICE. The difference is most pronounced for Case A in Fig. 2a with a deviation of over 30% whereas in the other cases the deviation is substantially lower. The turbulence model seems not to have a noticeable effect for the FENSAP-ICE results on the magnitude of the spike. The extent of the wet zone in Case A is quite similar, whereas for Case B and C the differences are significant. In the latter two cases, LEWICE predicts that the surface water film will never evaporate from the surface. The turbulent FENSAP-ICE results indicate that evaporation occurs eventually in all cases. With transition, full evaporation occurs only in Case A and partial evaporation in Case C.

The results for a fully evaporative anti-icing system are depicted in Fig. 3. The horizontal axis is cropped since outside of the impingement area the required anti-icing heat fluxes are zero. There were no significant differences between turbulent or transition modeling in FENSAP-ICE, so only one solution is shown. Overall, there is a much stronger overlap for the fully evaporative mode between LEWICE and FENSAP-ICE compared to running wet. Differences in the width and location of the impingement zone can be detected, in particular for Case C in Fig. 3c with the nonzero angle of attack. This is an indication of differences with the modeling of the droplet trajectories and impingement limits. The maximum surface temperatures required for full evaporation are 12°C, 19°C and 36°C for each of the cases, as indicated by LEWICE.

The total heats required for anti-icing (i.e. the areas under the curves in Fig. 2 & 3) are summarized in Table 2. For FENSAP-ICE, only the results with transition are shown. In addition, a value is given for the running wet heat required to keep the first 20% of the airfoil chord ($s/c < 0.2$) free of ice. The reason for this is because anti-icing

systems typically only protect the edge of a wing, where icing impacts are most significant. The overview confirms that both codes are predicting similar values, although variation occurs with average deviations ranging 3–42%.

Since Case A is displaying significant differences in both running wet and fully evaporative mode, it will be used to investigate the heat transfer on a 3D wing. FENSAP-ICE will fully resolve the full flow field around the wing in CFD, whereas LEWICE will only evaluate four 2D cross-sections. Figure 4 displays the running wet heat fluxes on the wing and the location of the 2D LEWICE cuts. The figure shows clearly the high required heat fluxes at the leading edge, and the transition area close to the trailing-edge. In Fig. 5, the required heat flux for every position along the span is shown for both running wet (RW) and fully evaporative (FE). For running wet, the required heat decreases along the span for both codes. This is explained by the decrease of the chord and thus the reduction of the heating area. The difference between the two codes seems to be a constant offset with an identical inclination until $y/b = 0.4$. From there till about $y/b = 0.9$ the FENSAP-ICE solution changes the inclination which seems to be correlated with changes in the transition location. At the very tip, a dip with a consequent increase in the FENSAP-ICE load curve occurs. The dip results from a change in the transition point, and the consequent increase from intensified heat transfer. Both effects are likely to originate from the wing tip vortex. For fully evaporative, both curves are nearly constant, which indicates that the size of the impingement area does not change significantly along the span. A steep increase of the required heat occurs at the wing tip with FENSAP-ICE, indicates vortex effects.

VI. Discussion

The objective of this paper is to investigate the differences between FENSAP-ICE and LEWICE for the simulation of icing protection systems. The results for anti-icing show that both codes are performing similarly, although differences do occur. The simulations indicate that for the running wet case, the presence of a laminar boundary layer is an important factor. This is not surprising, as convective heat transfer is significantly higher for turbulent boundary layers (Kays et al., 2005), thus requiring higher heat fluxes to keep the surface at a constant temperature. For the simulation of a UAV IPS, this is relevant because laminar flow characteristics are much more dominant at lower Reynolds numbers compared to general aviation. The sensitivity of the transition location to the boundary layer thickness and the surface roughness (i.e. from ice accretion or surface water film) should, therefore, be considered when simulating running wet anti-icing systems. From a simulation point of view, this is important, as laminar transition modeling with CFD remains a challenging task and may result in low fidelity results.

For both running wet and fully evaporative operation modes, LEWICE predicts 10-20% higher maximum required heat fluxes near the leading-edge compared to FENSAP-ICE. For the low-temperature case, a constant offset in the required heat fluxes appears which is likely to be related to differences in convective heat transfer modeling. This does not occur for the wet surfaces. Since only the latter is of interest from a design point of view, these differences may be less significant. All results illustrate that minor differences in the extent and location of the impingement limits between the two codes occur.

With regards to the design of an anti-icing system, several observations can be made. Both, a running wet and a fully evaporative system might be applicable for UAVs. The required heating zone temperatures for full evaporation at the leading-edge are significantly lower than for general aviation (often 100-200°C) due to the lower wind speeds. For running wet, the required heat fluxes can be reduced if only a part of the leading-edge area is protected. The comparison of required heats in Table 2 shows that ambient temperature plays a big role in the question which operation mode is the most efficient for UAVs. At moderate temperatures, a running wet system covering a limited area of the leading-edge will require significantly less energy than a fully evaporative system (Case B & C). At very low temperatures (Case A), however, an evaporative system has an advantage. This is because at low temperatures, heating a very small zone to a high temperature is more efficient than heating a large zone to a moderate temperature. The driving force is the difference between the required surface temperature and ambient conditions.

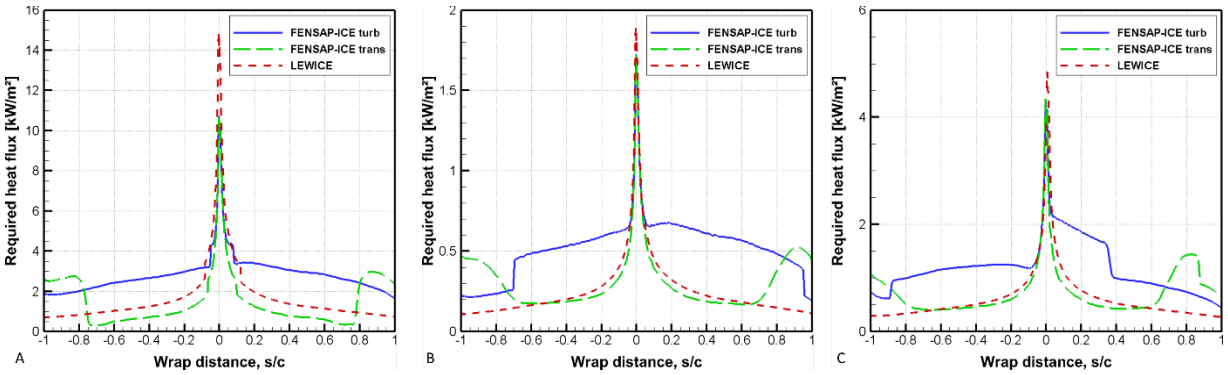

Fig. 2. Required anti-icing heat fluxes for running wet operation in FENSAP-ICE (turbulent & free transition) and LEWICE for all three icing test cases.

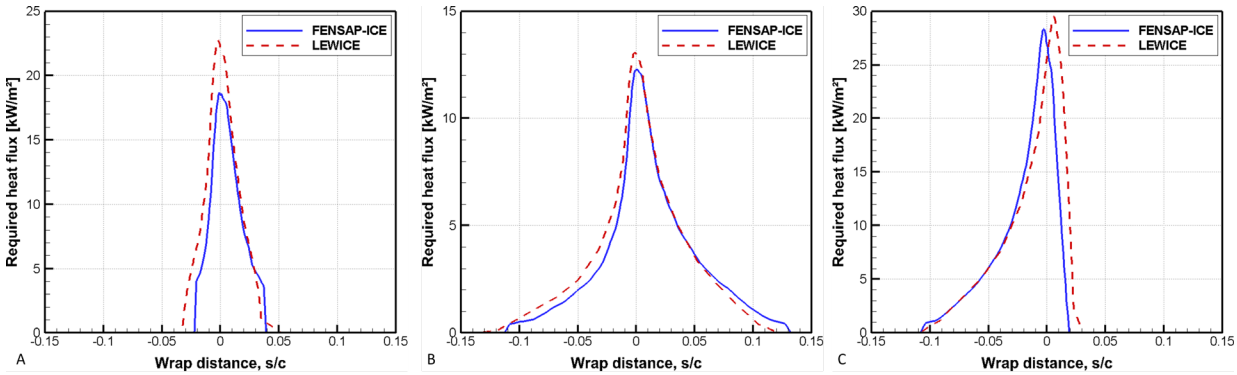

Fig. 3. Required anti-icing heat fluxes for fully evaporative operation in FENSAP-ICE and LEWICE for all three icing test cases.

A running wet system will compromise the aerodynamic performance due to runback icing. However, depending on the aerodynamic design, this might be tolerable to a certain degree. A fully evaporative system may lose its advantage when it needs to accommodate for varying impingement limits. In practice, the exact impingement limits are unknown, so a larger area must be heated which can result in significant amounts of waste heat. One effect that has not been studied is the impact of the surface temperature (here 0°C) for running wet cases. Higher temperatures will increase the evaporation rates and thus reduce the area to be protected, as well as reduce runback icing. In practice, the choice between the extent of heating area, surface temperature and allowable performance degradation must be carefully balanced for the design of an efficient anti-icing system.

The 3D investigations reveal effects at the wing-tip that are most likely related to the tip vortex, but these appear small in magnitude. This indicates that a full 3D resolution of a wing, which typically is related to high computational requirements, may not be required for simple wing geometries. It should be noted that the comparison between these two codes itself does not yield any insight into the fidelity of these codes. Without proper experimental validation, these tools are to be used with caution. Unfortunately, at this time there are no dedicated experiments on UAV IPS that would be suitable for validation.

VII. Conclusions

This paper compared two numerical icing codes, LEWICE and FENSAP-ICE, with regards to their capability to predict anti-icing heat requirements for UAV applications. Three cases have been chosen from on a parameter study based on the CFR 14, Part 25, Appendix C icing envelope for continuous maximum icing conditions. Simulations of a running wet and a fully evaporative system have been performed in 2D on the HQ/DS-2.5/13 airfoil. The results show the existence of three distinct thermodynamic regions. Both numerical codes predict generally similar results, although differences exist. For running wet, it was shown that the choice of the turbulence model (fully turbulent or transition) is significant. LEWICE assumed fully laminar flow over the entire airfoil, whereas FENSAP-ICE predicted

transition at approximately $s/c = 0.7$. It was shown that turbulent flow conditions increase evaporation rates and can lead to an earlier disappearance of the water layer compared to laminar conditions. This highlights the importance to understand the interactions between icing and transition for UAV airfoils, as well as the capability to model them accurately. The fully evaporative cases revealed that LEWICE is predicting higher required heat fluxes near the stagnation point and showed differences in the droplet impingement area. The comparison of the total required heat fluxes showed that depending on the ambient temperature, running wet or fully evaporative heating modes offer the lowest power requirements. This indicates that the identification of the critical icing design cases is an important task for the development of an UAV IPS.

Table 2. Total anti-icing heat fluxes for each 2D case as predicted by the numerical codes.

Required heat q [W/m]	Case A		Case B		Case C	
	LEWICE	FENSAP-ICE	LEWICE	FENSAP-ICE	LEWICE	FENSAP-ICE
Running wet total	1394	1266	205	256	458	607
Running wet 20%	674	439	92	82	205	198
Fully evaporative	299	236	338	311	531	464

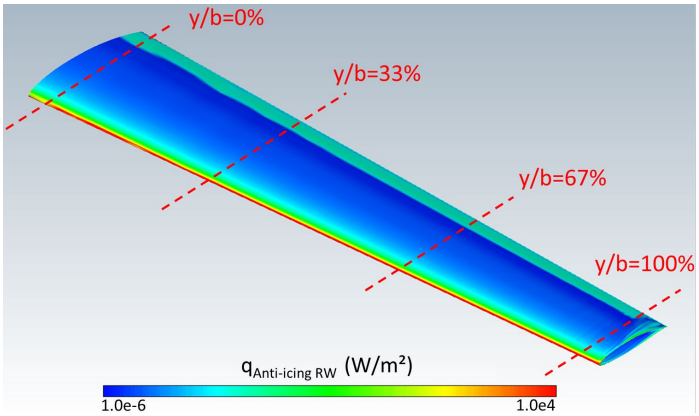

Fig. 4. FENSAP-ICE running wet solution for the 3D wing with the location of the cross-sections in LEWICE.

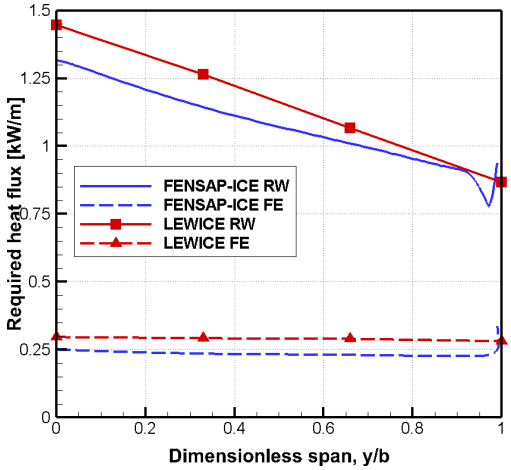

Fig. 5. Required anti-icing heat fluxes for Case A in FENSAP-ICE and LEWICE for the 3D wing.

Furthermore, the effect of 3D flow on anti-icing loads was investigated on a UAV wing. For this, 3D simulations have been carried out with FENSAP-ICE and compared to corresponding 2D cross-sections with LEWICE. The results show that FENSAP-ICE predicts similar trends as LEWICE for the fully evaporative mode. Differences occur in the running wet case are linked to the simulation of the transition location. In addition, 3D effects at the wing tip can be observed for both modes, likely to be related to the wing-tip vortex. The effects are limited in magnitude and may be neglectable for simple wing geometries.

In summary, the differences between the two codes are moderate. The results show that the boundary layer conditions and transition location have a major influence on the required heat fluxes for running wet conditions in FENSAP-ICE. This indicates that some focus should be spent on further studies on the effect of initial surface roughness and water film thickness interactions with the boundary layer. 3D effects appear to be of limited magnitude but may also require closer investigation. Generally, the results suggest that the faster LEWICE tool for the design of UAV IPS may be possible. However, it is important to note that both codes are not validated for predicting IPS loads for the Reynolds number regime of this study. Therefore, the fidelity of the codes cannot be evaluated based on this work. Further experimental work is necessary to build more confidence in these numerical methods.

Acknowledgments

This project has received funding from the Centre for Integrated Remote Sensing and Forecasting for Arctic Operations (CIRFA) under grant number 237906. The research was also funded by the Research Council of Norway through the Centre of Excellence funding scheme, grant number 223254 NTNU AMOS. I would like to thank my supervisor Tor Arne Johansen for his support of my work.

References

Battisti, L.: Wind Turbines in Cold Climates, Springer., 2015.

Bragg, M. B., Broeren, A. P. and Blumenthal, L. A.: Iced-airfoil aerodynamics, Prog. Aerosp. Sci., 41(5), 323–362, doi:10.1016/j.paerosci.2005.07.001, 2005.

Drela, M.: XFOIL: An Analysis and Design System for Low Reynolds Number Airfoils, in Low Reynolds Number Aerodynamics, edited by T. J. Mueller, pp. 1–12, Springer Berlin Heidelberg, Berlin, Heidelberg., 1989.

Federal Aviation Administration: 14 CFR Parts 25 and 29, Appendix C, Icing Design Envelopes, DOT/FAA/AR-00/30., 2002.

Gent, N. P. D. and Cansdale, J. T.: Aircraft icing, Philos. Trans. R. Soc. London A Math. Phys. Eng. Sci., 358, 2000.

Goraj, Z.: An Overview of the Deicing and Antiicing Technologies with Prospects for the Future, 24Th Int. Congr. Aeronaut. Sci., 1–11, 2004.

Habashi, W. G., Aubé, M., Baruzzi, G., Morency, F., Tran, P. and Narramore, J. C.: FENSAP-ICE : A Fully-3D in-Flight Icing Simulation System for Aircraft , Rotorcraft and UAVs, in 24th International Congress of the Aeronautical Sciences, ICAS. [online] Available from: http://www.icas.org/ICAS_ARCHIVE/ICAS2004/PAPERS/608.PDF, 2004.

Hann, R.: Opportunities and Challenges for Unmanned Aerial Vehicles (UAVs) in the Arctic, in 13th ArcticNet Annual Scientific Meeting., 2017.

Hann, R.: UAV Icing: Comparison of LEWICE and FENSAP-ICE for Ice Accretion and Performance Degradation, in 2018 Atmospheric and Space Environments Conference, AIAA Aviation, Atlanta., 2018.

Hann, R., Wenz, A., Gryte, K. and Johansen, T. A.: Impact of atmospheric icing on UAV aerodynamic performance, in 2017 Workshop on Research, Education and Development of Unmanned Aerial Systems, RED-UAS 2017, pp. 66–71, Linköping., 2017.

Kays, W. M., Crawford, M. E. and Weigand, B.: Convective heat and mass transfer, McGraw-Hill., 2005.

Morency, F., Beaugendre, H., Baruzzi, G. and Habashi, W.: FENSAP-ICE - A comprehensive 3D simulation system for in-flight icing, 15th AIAA Comput. Fluid Dyn. Conf., (June), doi:10.2514/6.2001-2566, 2001.

Quabeck, H.: HQ-Profile für den Modellflug, HQ-Modellflugliteratur., 2014.

Reid, T., Baruzzi, G. S., Ozcer, I. A. and Habashi, W. G.: FENSAP-ICE: 3D Simulation, and Validation, of De-icing with Inter-cycle Ice Accretion, , doi:10.4271/2011-38-0102, 2011.

Schlichting, H.: Boundary-Layer Theory, , doi:10.1007/978-1-4757-3069-2_9, 1968.

Siquig, A.: Impact of Icing on Unmanned Aerial Vehicle (UAV) Operations, Naval Environmental Prediction Research Facility., 1990.

Sørensen, K. L.: Autonomous Icing Protection Solution for Small Unmanned Aircraft, NTNU. [online] Available from: http://folk.ntnu.no/torarnj/Kim_thesis_12_09_2016.pdf, 2016.

Szilder, K. and McIlwain, S.: In-Flight Icing of UAVs - The Influence of Reynolds Number on the Ice Accretion Process, SAE Technical Paper 2011-01-2572., 2011.

Szilder, K. and Yuan, W.: In-flight icing on unmanned aerial vehicle and its aerodynamic penalties, Prog. Flight Phys., 9, 173–188, doi:10.1051/eucass/201709173, 2017.

Tran, P., Baruzzi, G., Tremblay, F., Benquet, P., Habashi, W. G., Petersen, P. B., Liggett, M. W. and Fiorucci, S.: FENSAP-ICE applications to unmanned aerial vehicles (UAV), in 42nd AIAA Aerospace Sciences Meeting and Exhibit, pp. 390–402., 2004.

Whalen, EA; Broeren, AP; Bragg, M.: Characteristics of Runback Ice Accretions and Their Aerodynamic Effects, , (April), 2007.

Williams, N., Benmeddour, A., Brian, G. and Ol, M.: The effect of icing on small unmanned aircraft low Reynolds number airfoils, in 17th Australian International Aerospace Congress, AIAC, Melbourne., 2017.

Wright, W.: User's Manual for LEWICE Version 3.2, NASA/CR—2008-214255., 2008.

Wright, W. and Rutkowski, A.: Validation Results for LEWICE 2.0, NASA/CR—1999-208690., 1999.